Vol 17 No 6, June 2008
1674-1056/2008/17(06)/2304-07

Chinese Physics B

© 2008 Chin. Phys. Soc.
and IOP Publishing Ltd

A phase analysis of vorticity vectors associated with tropical convection*

Cui Xiao-Peng(崔晓鹏)†

Laboratory of Cloud-Precipitation Physics and Severe Storms (LACS), Institute of Atmospheric Physics, Chinese Academy of Sciences, Beijing 100029, *China*

(Received 20 June 2007; revised manuscript received 29 January 2008)

Three new vorticity vectors have been proposed by Gao *et al* to study the two-dimensional tropical convection. In the present paper, phase relations between surface rain rate and the vorticity vectors are analysed with the calculations of lag correlation coefficients based on hourly zonally-averaged mass-integrated cloud-resolving simulation data. The cloud-resolving model is integrated with the vertical velocity, zonal wind, horizontal thermal and moisture advections, and sea surface temperature observed and derived from tropical ocean global atmosphere – coupled ocean atmosphere response experiment (TOGA-COARE) for 10 days. Maximum local increase of the vertical component of the convective vorticity vector leads maximum surface rain rate by 2 hours mainly due to the interaction between vorticity and zonal gradient of ice heating. While maximum local increase of the vertical component of the moist vorticity vector leads maximum surface rain rate by 2 hours mainly because of the interaction between zonal specific humidity gradient and zonal buoyancy gradient. And the maximum local decrease of the zonal component of the dynamic vorticity vector leads maximum surface rain rate by 2 hours mainly due to the interactions between vorticity and vertical pressure gradient as well as vorticity and buoyancy.

Keywords: phase analysis, vorticity vectors, tropical convection, cloud-resolving model
PACC: 9260N, 9260J, 9260X, 9260E

1. Introduction

Dry and moist potential vorticity has been an important parameter in meteorology for decades, and the analysis of it has led to a better understanding of dynamic and thermodynamic processes associated with weather systems such as midlatitude frontal systems and tropical squall lines.[1−15] However, the potential vorticity could be zero for a two-dimensional (2D) equatorial flow. To solve this problem, Gao *et al*[16] introduced a convective vorticity vector ($\frac{\boldsymbol{\xi} \times \nabla \theta_{\mathrm{e}}}{\rho}$, CVV) to analyse the 2D tropical convection. Their analysis of zonally-averaged and mass-integrated quantities showed that the correlation coefficient between the vertical component of the CVV and the sum of the cloud hydrometeor mixing ratios (0.81) is much larger than that between the zonal component and the sum (0.18). This indicates that the vertical component of the CVV is closely associated with the tropical convection. Since the vertical component of the CVV is determined by the covariance between the zonal component of vorticity and the zonal gradient of equivalent potential temperature (the zonal component of vorticity represents the secondary circulation in horizontal–vertical framework that is directly associated with vertical motion in tropical convections), the above higher coefficient is easy to understand. So the vertical component of the CVV could be regarded as an indicator of cloud (hydrometeor) development. They further derived a tendency equation for the vertical component of the CVV, analysed the zonally-averaged and mass-integrated tendency budget. They found that the tendency is mainly determined by the interaction between vorticity and zonal gradient of cloud heating. Considering the important role of water vapour in tropical convective development, Gao *et al*[17] defined a moist vorticity vector ($\frac{\xi \times \nabla q_{\mathrm{v}}}{\rho}$, MVV). The MVV is similar to the CVV except that the equivalent potential temperature is replaced by specific humidity in the MVV, since the contrast of water vapour is much important than that of temperature in the tropics. Their study showed

*Project supported by the National Natural Science Foundation of China (Grant Nos 40433007 and 40505012), the Knowledge Innovation Program of the Chinese Academy of Sciences (IAP07214) and "Outstanding Oversea Scholars" project (Grant No 2005-2-17).

†E-mail: xpcui@mail.iap.ac.cn

that the vertical component of the MVV has a larger correlation coefficient (0.78) with the sum of the cloud hydrometeor mixing ratios than the zonal component has (0.32), which is similar to the result of the CVV. The tendency of the vertical component of the MVV is mainly determined by the interaction between vorticity and zonal gradient of condensational/depositional heating. They also constructed a dynamic vorticity vector[17] ($\frac{\boldsymbol{\xi} \times \boldsymbol{V}}{\rho}$, DVV). The vertical component of the DVV is in phase with the sum of the mixing ratios (0.52) whereas the zonal component is out of phase with the sum of the mixing ratios (–0.62). The variation tendency of the zonal component of the DVV is mainly controlled by the interactions among vorticity, buoyancy, and vertical pressure gradient. Whereas the tendency of the vertical component is mainly determined by the interaction between vorticity and zonal pressure gradient. Ping *et al*[18] analysed the horizontal distributions of surface rain rate and vertical component of the DVV and found that their correlation is not statistically significant, while the zonal component of the DVV is associated with the covariance between the zonal component of vorticity and vertical velocity. Since the zonal component of vorticity is associated with the secondary circulation, the zonal component of the DVV represents the secondary circulation of the tropical convection, which is a direct cloud and rainfall producer as discussed above.

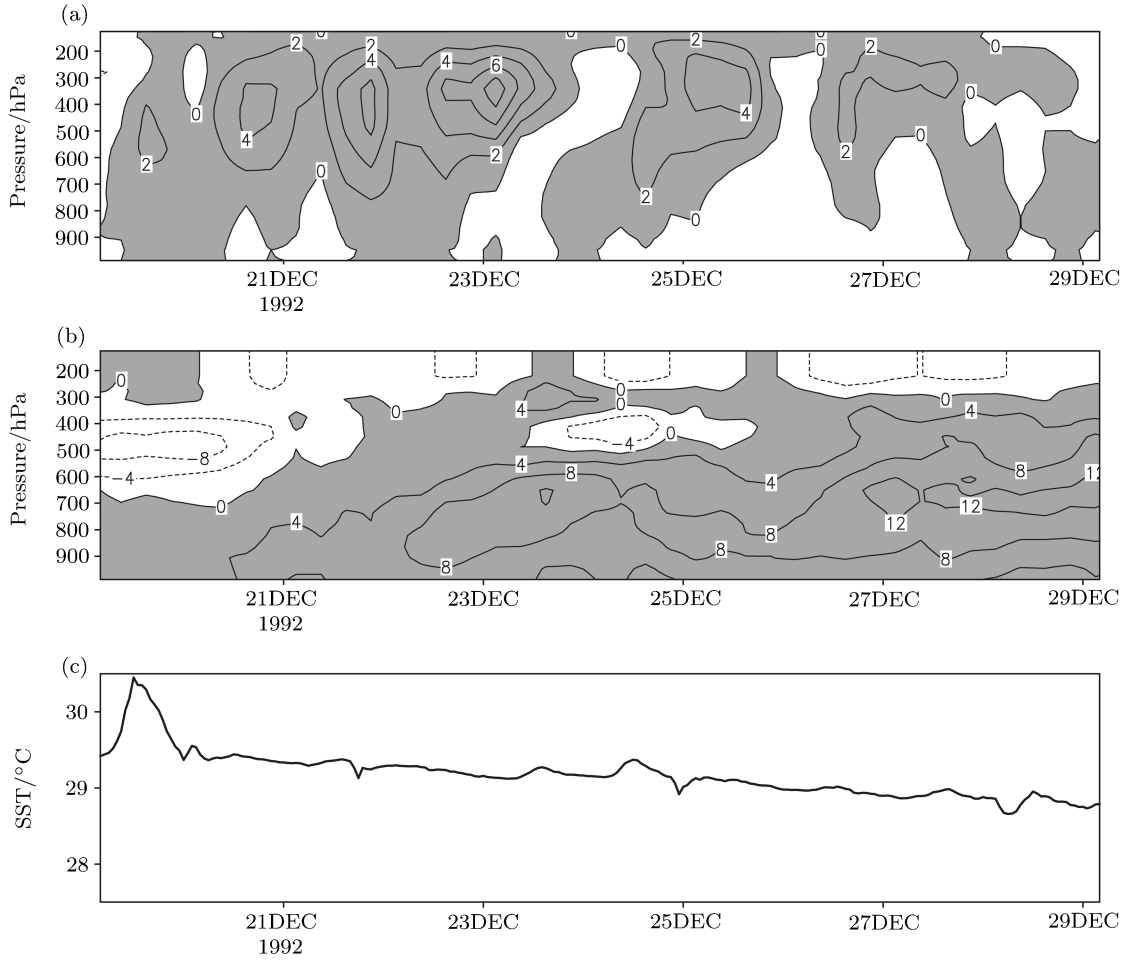


Fig.1. Temporal and vertical distributions of vertical velocity (a), zonal wind (b), and time series of sea surface temperature (c), observed and derived from TOGA COARE for the 10-day period. Upward motion in (a) and westerly wind in (b) are shaded. Units of vertical velocity, zonal wind, and sea surface temperature are cm s^{-1}, m s^{-1}, and °C, respectively.

To detect the physical processes that control the convective development and produce surface rainfall, the phase relations between the vorticity vectors and surface rain rate are investigated in this study based on hourly zonal-mean data from a $2D$ cloud-resolving simulation. The central questions to be answered are:

Are there phase differences between the vorticity vectors and surface rain rate? What physical processes determine these phase differences? In the next section the model, forcing, and experiment are briefly described. The results are presented in section 3, and the summary is given in section 4.

2. Model

The cloud-resolving model used in this study has been originally developed by Soong and Ogura,[19] Soong and Tao,[20] and Tao and Simpson.[21] The 2D version of the model used by Sui *et al*[22,23] and further modified by Li *et al*[24] is what is used in this study. The governing equations and the model in details can be found in Li *et al*[24,25] Several 2D cloud-resolving models have successfully simulated atmospheric thermodynamic profiles, cloud properties, and precipitation in the tropics during the global atmospheric research programme Atlantic tropical experiment[26,27] and tropical ocean global atmosphere coupled ocean-atmosphere response experiment (TOGA COARE).[16,17,24,25,28−34]

The model is forced by zonally-uniform vertical velocity, zonal wind, and thermal and moisture advection, based on TOGA COARE observations within the intensive flux array (IFA) region. Calculations are based on a constrained, variational method applied to column-integrated budgets of mass, heat, moisture and momentum as proposed by Zhang and Lin.[35] Hourly sea surface temperature (SST) at the improved meteorological (IMET) surface mooring buoy (1.75°S, 156°E)[36] is also imposed in the model. The model is integrated from 0400 LST 19 December 1992 to 0400 LST 29 December 1992 (10 days total). Figure 1 shows the time evolution of the vertical distribution of large-scale forcing (vertical velocity, zonal wind and time series of SST during the 10-day period) used in the simulation. In this model, the horizontal boundary is periodic, and the horizontal domain is 768 km with a horizontal grid resolution of 1.5 km. The vertical grid resolution ranges from about 200 m near the surface to about 1 km near 100 hPa. The time step is 12 s.

3. Results

Since the vertical components of the CVV, the MVV and the zonal component of the DVV have close relation with tropical convection as mentioned above, only these three components will be discussed below. Vertical components of the CVV (C_z),[16] the MVV (M_z)[17] and the zonal component of the DVV (D_x)[17] can be expressed, respectively, as

$$C_z = -\frac{\zeta}{\overline{\rho}}\frac{\partial \theta_{\mathrm{e}}}{\partial x}, \tag{1a}$$

$$M_z = -\frac{\zeta}{\overline{\rho}}\frac{\partial q_{\mathrm{v}}}{\partial x}, \tag{1b}$$

$$D_x = -\frac{w\zeta}{\overline{\rho}}, \tag{1c}$$

where $\zeta = \dfrac{\partial u}{\partial z} - \dfrac{\partial w}{\partial x}$, u and w are the zonal and vertical wind components, respectively, x and z the zonal and vertical coordinates, respectively; θ_{e} is the equivalent potential temperature; q_{v} is the specific humidity of water vapour; ρ is the air density; overbar is a zonal-mean.

Figure 2 shows the lag correlation coefficients between zonal-mean surface rain rate $[P_{\mathrm{s}}]$ and $\dfrac{\partial [C_z]}{\partial t}$, $[P_{\mathrm{s}}]$ and $\dfrac{\partial [M_z]}{\partial t}$, as well as $[P_{\mathrm{s}}]$ and $\dfrac{\partial [D_x]}{\partial t}$($[F] = \sum_{i=1}^{512} \dfrac{1}{512} \int_0^{z_{\mathrm{T}}} \overline{\rho} F_i \mathrm{d}z$, z_{t} is the height of top atmosphere). Positive lag hour denotes that maximum $\dfrac{\partial [C_z]}{\partial t}$ and $\dfrac{\partial [M_z]}{\partial t}$ lead maximum $[P_{\mathrm{s}}]$, whereas negative lag hour denotes that maximum $\dfrac{\partial [D_x]}{\partial t}$ lags behind the maximum $[P_{\mathrm{s}}]$. Lag correlation coefficients between $[P_{\mathrm{s}}]$ and $\dfrac{\partial [C_z]}{\partial t}$, and $[P_{\mathrm{s}}]$ and $\dfrac{\partial [M_z]}{\partial t}$ are similar since the water vapour plays a dominant role in the development of tropical convection.[29,30] Their maximum positive lag correlation coefficients (0.32) occur at lag hour 2 whereas their maximum negative lag correlation coefficients (–0.33) appear at about lag hour –1–−2, which exceed 99% confidence level (0.18). This indicates that maximum local increases of $[C_z]$ and $[M_z]$ occur 2 h before $[P_{\mathrm{s}}]$ reaches maximum, whereas maximum local decreases of $[C_z]$ and $[M_z]$ appear 1–2 h after $[P_{\mathrm{s}}]$ reaches maximum. Since the vertical components of the CVV and MVV could be regarded as an indicator of the development of cloud (hydrometeors),[16,17] the above phase relations mean that the development of cloud (hydrometeors) will reach its maximum just about 2 h before the surface rain rate reaches its maximum, and the decay of the cloud will reach its maximum just about 1–2 h after the maximum surface rain rate. This is identical to the results in Ref.[33]. The maximum negative lag

correlation coefficient between $[P_s]$ and $\frac{\partial[D_x]}{\partial t}$ (-0.23) appears at lag hour 2 whereas the maximum positive lag correlation coefficient (0.30) occurs at lag hour –1. This suggests that the maximum local decrease of $[D_x]$ occurs 2 h ahead of maximum $[P_s]$, whereas the maximum local increase of $[D_x]$ appears 1 hour behind the maximum $[P_s]$. It is interesting to notice that the lag correlation coefficients between $[P_s]$ and $\frac{\partial[D_x]}{\partial t}$, and $[P_s]$ and $\frac{\partial[C_z]}{\partial t}$ (or between $[P_s]$ and $\frac{\partial[M_z]}{\partial t}$) are roughly symmetric about zero (Fig.2), implying that the zonal component of the DVV and vertical components of CVV/MVV may set a dynamic-thermodynamic coupling for the tropical convective development. The definition of the zonal component of the DVV (refer to Eq(1c)) shows that the D_x is associated with the covariance of the vertical velocity (w) and the zonal component of vorticity (It should be noticed that there is a negative signal in the definition of the D_x). Since the zonal component of vorticity is associated with the secondary circulation,[17] the zonal component of the DVV represents the secondary circulation of the tropical convection, which is a direct cloud and rainfall producer. Thus the maximum local decrease of $[D_x]$, occurring 2 h ahead of maximum $[P_s]$, means that the covariance of the vertical velocity and secondary circulation will reach its maximum 2 h before the maximum surface rain rate. And the maximum local increase of $[D_x]$ means that the covariance of the vertical velocity and secondary circulation will reach its minimum 1 hour after the maximum surface rain rate. Thus, maximum $\frac{\partial[C_z]}{\partial t}$ and $\frac{\partial[M_z]}{\partial t}$ and minimum $\frac{\partial[D_x]}{\partial t}$ lead maximum $[P_s]$ by 2 h. The maximum to maximum or minimum to minimum lag correlation coefficients are about 9 h apart. This indicates that the life span of simulated tropical convection is 9 h, which is consistent with the results in Ref.[30].

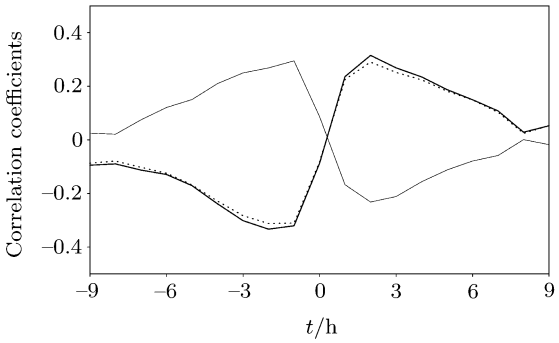


Fig.2. Lag correlation coefficients between zonal-mean surface rain rate $[P_s]$ and $\frac{\partial[C_z]}{\partial t}$ (dark solid line), $[P_s]$ and $\frac{\partial[M_z]}{\partial t}$ (dotted line), $[P_s]$ and $\frac{\partial[D_x]}{\partial t}$ (light solid line).

The tendency equations of the vorticity vectors are derived by Gao *et al*[16,17] and can be expressed as

$$\frac{\partial[C_z]}{\partial t} = \underbrace{\left[\frac{\zeta}{\overline{\rho}}\left(\frac{\partial u}{\partial x}\frac{\partial \theta_e}{\partial x} + \frac{\partial w}{\partial x}\frac{\partial \theta_e}{\partial z}\right)\right]}_{CZ1} + \underbrace{\left[\frac{1}{\overline{\rho}}\frac{\partial \theta_e}{\partial x}\frac{\partial B}{\partial x}\right]}_{CZ2} - \underbrace{\frac{L_f}{c_p}\left[\frac{\zeta}{\overline{\rho}}\frac{\partial}{\partial x}\left(\frac{P_{18}\theta_e}{T}\right)\right]}_{CZ3} - \underbrace{\frac{1}{c_p}\left[\frac{\zeta}{\overline{\rho}}\frac{\partial}{\partial x}\left(\frac{Q_R\theta_e}{T}\right)\right]}_{CZ4}, \tag{2a}$$

$$\frac{\partial[M_z]}{\partial t} = \underbrace{\left[\frac{\zeta}{\overline{\rho}}\left(\frac{\partial u}{\partial x}\frac{\partial q_v}{\partial x} + \frac{\partial w}{\partial x}\frac{\partial q_v}{\partial z}\right)\right]}_{MZ1} + \underbrace{\left[\frac{1}{\overline{\rho}}\frac{\partial q_v}{\partial x}\frac{\partial B}{\partial x}\right]}_{MZ2} + \underbrace{\left[\frac{\zeta}{\overline{\rho}}\frac{\partial}{\partial x}(S_{qv})\right]}_{MZ3}, \tag{2b}$$

$$\frac{\partial[D_x]}{\partial t} = -\underbrace{\left[\frac{w}{\overline{\rho}}\frac{\partial B}{\partial x}\right]}_{DX1} + \underbrace{\left[\frac{\zeta B}{\overline{\rho}}\right]}_{DX2} - \underbrace{c_p\left[\frac{\zeta}{\overline{\rho}}\frac{\partial}{\partial z}(\overline{\theta\pi})\right]}_{DX3}. \tag{2c}$$

The detailed derivations and symbols of Eqs.(2) can be found in Refs.[16] and [17].

To elucidate the physical processes responsible for the phase differences between the surface rain rate and the vorticity vectors, the lag correlation coefficients between the surface rain rate and the budgets of the vorticity vectors are calculated. For example, the linear correlation coefficient (C_{CZT,P_s}) between the tendency ($[CZT] = [CZ1] + [CZ2] + [CZ3] + [CZ4]$) and

$[P_s]$ can be expanded into

$$C_{CZT,P_s} = \sum_{i=1}^{4} \frac{\sigma_{CZi}}{\sigma_{CZT}} C_{CZi,P_s}, \tag{3}$$

where σ is a standard deviation; $\frac{\sigma_{CZi}}{\sigma_{CZT}} C_{CZi,P_s}$ is a weighted linear correlation coefficient between $[CZi]$ and $[P_s]$.

Figure 3 shows weighted lag correlation coefficients between $[P_s]$ and the budget of $[C_z]$. $[CZ1]$ is in phase with $[P_s]$ whereas $[CZ2]$ is out of phase with $[P_s]$, whose lag correlation coefficients reach maximum and minimum at lag hour 0, respectively. The weighted lag correlation coefficient between $[P_s]$ and $[CZ4]$ is negligibly small. The weighted lag correlation coefficient between $[P_s]$ and $[CZ3]$ reach maximum (0.17) at lag hour 2, which coincides with the maximum lag correlation coefficient between $[P_s]$ and $\frac{\partial[C_z]}{\partial t}$. Note that the lag correlation coefficient between $[P_s]$ and $[CZ3]$ is marginally about 99% confidence level. The lag correlation coefficient between $[P_s]$ and $[CZ3]+[CZ1]$ reaches maximum (0.35) at lag hour 2. It suggests that the interactions among zonal velocity (u) gradient and zonal equivalent potential temperature gradient and vorticity or the interactions among zonal velocity (w) gradient and vertical equivalent potential temperature gradient and vorticity (the term $CZ1$ in Eq.(2a)) also play a role in determining the phase difference at lag hour 2. The maximum negative weighted lag correlation coefficient between $[P_s]$ and $[CZ3]$ (–0.44) occurs at lag hour –1, which fully account for the maximum negative lag correlation coefficient between $[P_s]$ and $\frac{\partial[C_z]}{\partial t}$. Thus, the

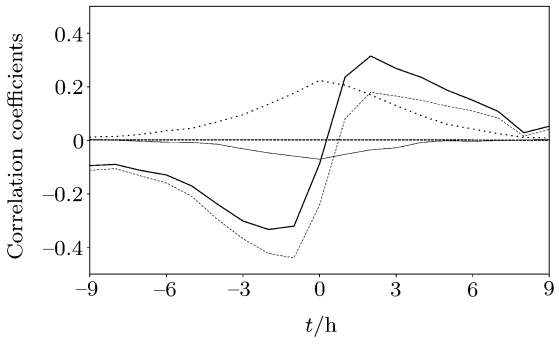


Fig.3. Lag correlation coefficient between $[P_s]$ and $\frac{\partial[C_z]}{\partial t}$ (dark solid line), and weighted lag correlation coefficients between $[P_s]$ and $[CZ1]$ (dotted line), $[P_s]$ and $[CZ2]$ (light solid line), $[P_s]$ and $[CZ3]$ (light dashed line), and $[P_s]$ and $[CZ4]$ (dark dashed line).

maximum positive $\frac{\partial[C_z]}{\partial t}$ leads maximum $[P_s]$ by 2 h and the maximum negative $\frac{\partial[C_z]}{\partial t}$ lags behind the maximum $[P_s]$ by 1 hour, mainly due to the interaction between vorticity and the zonal gradient of ice heating, and $[CZ1]$ provides an important modification.

Figure 4 shows the weighted lag correlation coefficients between $[P_s]$ and the budget of $[M_z]$. Since the maximum positive weighted lag correlation coefficient between $[P_s]$ and $[MZ2]$ (0.54) occurs at lag hour 0, the maximum negative weighted lag correlation coefficient between $[P_s]$ and $[MZ3]$ (–0.75) appears at lag hour –1, and the weighted lag correlation coefficient between $[MZ1]$ and $[P_s]$ is negligibly small, the weighted lag correlation coefficient between $[P_s]$ and $[MZ2]$ can account for the maximum positive lag correlation coefficient between $[P_s]$ and $\frac{\partial[M_z]}{\partial t}$, whereas the negative weighted lag correlation coefficient between $[P_s]$ and $[MZ3]$ can explain the maximum negative lag correlation coefficient between $[P_s]$ and $\frac{\partial[M_z]}{\partial t}$. Thus, the maximum positive $\frac{\partial[M_z]}{\partial t}$ leads maximum $[P_s]$ by 2 h mainly due to the interactions between the zonal specific humidity gradient and zonal buoyancy gradient; and the maximum negative $\frac{\partial[M_z]}{\partial t}$ lags behind the maximum $[P_s]$ by 1 hour mainly due to the interaction between the vorticity and the zonal condensation/deposition gradient.

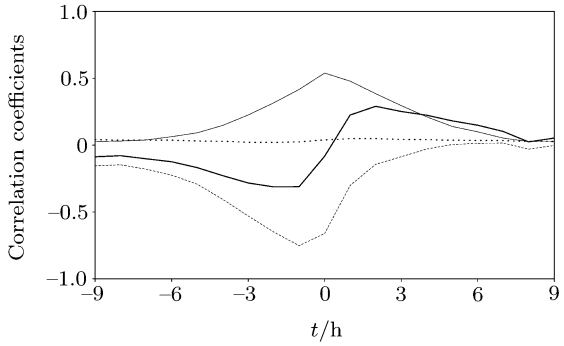


Fig.4. Lag correlation coefficient between $[P_s]$ and $\frac{\partial[M_z]}{\partial t}$ (dark solid line), and weighted lag correlation coefficients between $[P_s]$ and $[MZ1]$ (dotted line), $[P_s]$ and $[MZ2]$ (light solid line), and $[P_s]$ and $[MZ3]$ (dashed line).

It should be pointed out that although the vertical components of the CVV and MVV have similar variations in both phases and magnitudes due to the dominant role of water vapour in tropical convection, they may be different from each other in the following aspect. The interaction between the vorticity and the zonal gradient of ice heating primarily determines the

local change of the vertical component of the CVV,[16] and the maximum positive and negative lag correlation coefficients with the surface rain rate. The interaction between the vorticity and the zonal gradient of cloud (water/ice) heating controls the local change of the vertical component of the MVV[17] and the maximum negative lag correlation coefficient with the surface rain rate. And the interaction between the zonal specific humidity gradient and the zonal buoyancy gradient is mainly responsible for the maximum positive lag correlation between the surface rain rate and the local increase of the vertical component of the MVV.

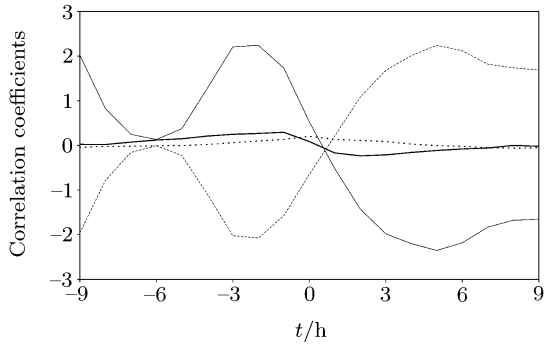


Fig.5. Lag correlation coefficient between $[P_s]$ and $\frac{\partial[D_x]}{\partial t}$ (dark solid line), and weighted lag correlation coefficients between $[P_s]$ and $[DX1]$ (dotted line), $[P_s]$ and $[DX2]$ (light solid line), and $[P_s]$ and $[DX3]$ (dashed line).

Figure 5 shows the weighted lag correlation coefficients between $[P_s]$ and the budget of $[D_x]$. The weighted lag correlation coefficients between $[P_s]$ and $[DX2]$ as well as $[P_s]$ and $[DX3]$ show large variations with a magnitude more than 2. They are nearly out of phase and largely cancel each other out. We can see that the weighted lag correlation coefficient between $[P_s]$ and $[DX1]$ is relatively small. Also the maximum positive weighted lag correlation coefficient between $[P_s]$ and $[DX2]+[DX3]$ occurs at lag hour −1, whereas the maximum negative lag correlation coefficient appears at lag hour 2. This indicates that the maximum local decrease of $[D_x]$ occurs 2 h ahead of the maximum $[P_s]$, and the maximum local increase of $[D_x]$ appears 1 h behind the maximum $[P_s]$ mainly due to the interactions between vorticity and vertical pressure gradient as well as vorticity and buoyancy.

4. Summary

Gao *et al*[16,17] proposed three new vorticity vectors and found that they are highly correlated with two-dimensional tropical convection. In this paper, we have calculated lag correlation coefficients to study the phase relations between the vorticity vectors and the surface rain rate in the tropical deep convection by using hourly zonally-averaged mass-integrated cloud-resolving simulation data. The model is integrated with the vertical velocity, zonal wind, horizontal thermal and moisture advections, and sea surface temperature observed and derived from TOGA-COARE for 10 days.

Maximum local increase of the vertical component of the CVV[16] leads maximum surface rain rate by 2 h due to the interaction between vorticity and zonal gradient of ice heating, as well as the interaction among zonal velocity (u) gradient and zonal equivalent potential temperature gradient and vorticity, or the interaction among zonal velocity (w) gradient and vertical equivalent potential temperature gradient and vorticity. Whereas the maximum local decrease of the vertical component of the CVV lags behind the maximum surface rain rate by 1 hour mainly due to the interaction between vorticity and zonal gradient of ice heating. The maximum local increase of the vertical component of the MVV[17] leads maximum surface rain rate by 2 h mainly due to the interaction between zonal specific humidity gradient and zonal buoyancy gradient, whereas the maximum local decrease lags behind the maximum surface rain rate by 1 hour mainly due to the interaction between vorticity and zonal condensation/deposition gradient.

Maximum local decrease of the zonal component of the DVV[17] leads maximum surface rain rate by 2 h, and the maximum local increase lags behind the maximum surface rain rate by 1 hour mainly due to the interaction between vorticity and vertical pressure gradient, as well as that between vorticity and buoyancy.

References

[1] Bennetts D A and Hoskins B J 1979 *Quart. J. Roy. Meteor. Soc.* **105** 945
[2] Emanuel K A 1979 *J. Atmos. Sci.* **36** 2425
[3] Danielsen E F and Hipskind R S 1980 *J. Geophys. Res.* **85**(C1) 393
[4] Thorpe A J 1985 *J. Atmos. Sci.* **42** 397
[5] Hoskins B J and Berrisford P 1988 *Weahter* **43** 122
[6] Xu Q 1992 *J. Atmos. Sci.* **49** 629

[7] Montgomery M T and Farrell B F 1993 *J. Atmos. Sci.* **50** 285
[8] Cao Z and Cho H 1995 *J. Atmos. Sci.* **52** 3263
[9] Cho H and Cao Z 1998 *J. Atmos. Sci.* **55** 595
[10] Gao S, Lei T and Zhou Y 2002 *Chin. Phys. Lett.* **19** 878
[11] Wang P and Dai X 2005 *Acta Phys. Sin.* **54** 4961 (in Chinese)
[12] Cao J, Gao S and Zhou Y 2008 *Acta Phys. Sin.* **57** (in Chinese)
[13] Cui X, Wu G and Gao S 2002 *Acta Meteor. Sin.* **60** 385 (in Chinese)
[14] Cui X, Gao S and Wu G 2003 *Chin. Phys. Lett.* **20** 167
[15] Cui X, Gao S and Wu G 2003 *Advs. Atmos. Sci.* **20** 825
[16] Gao S, Ping F, Li X and Tao W K 2004 *J. Geophys. Res.* **109** D14106 doi:10.1029/2004JD004807
[17] Gao S, Cui X, Zhou Y, Li X and Tao W K 2005 *J. Geophys. Res.* **110** D17104 doi:10.1029/2004JD005675
[18] Ping F, Luo Z and Li X 2007 *Atmos. Res.* doi:10.1016/j.atmosres.2007.11.027
[19] Soong S T and Ogura Y 1980 *J. Atmos. Sci.* **37** 2035
[20] Soong S T and Tao W K 1980 *J. Atmos. Sci.* **37** 2016
[21] Tao W K and Simpson J 1993 *Terr. Atmos. Oceanic Sci.* **4** 35
[22] Sui C H, Lau K M, Tao W K and Simpson J 1994 *J. Atmos. Sci.* **51** 711
[23] Sui C H, Li X and Lau K M 1998 *J. Atmos. Sci.* **55** 2345
[24] Li X, Sui C H, Lau K M and Chou M D 1999 *J. Atmos. Sci.* **56** 3028
[25] Li X, Sui C H and Lau K M 2002 *Mon. Wea. Rev.* **130** 2481
[26] Xu K M and Randall D A 1996 *J. Atmos. Sci.* **53** 3710
[27] Grabowski W W, Wu X and Moncrieff M W 1996 *J. Atmos. Sci.* **53** 3684
[28] Wu X, Grabowski W W and Moncrieff M W 1998 *J. Atmos. Sci.* **55** 2693
[29] Li X, Sui C H and Lau K M 2002 *J. Meteor. Soc. Japan* **80** 205
[30] Li X, Sui C H and Lau K M 2002 *J. Atmos. Sci.* **59** 1712
[31] Li X, Sui C H, Lau K M and Tao W K 2004 *Meteor. Atmos. Phys.* doi: 10.1007/s00703-004-0088-5
[32] Gao S, Ping F and Li X 2005 *Meteor. Atmos. Phys.* doi: 10.1007/s00703-005-0108-5
[33] Gao S, Cui X, Zhu Y and Li X 2005 *J. Geophys. Res.* **110** D10202 doi: 10.1029/2004JD005467
[34] Gao S, Ping F and Li X 2005 *Atmos. Res.* doi: 10.1016/j.atmosres.2005.04.002
[35] Zhang M H and Lin J L 1997 *J. Atmos. Sci.* **54** 1503
[36] Weller R A and Anderson S P 1996 *J. Climate* **9** 1959